Chapter 10

Interferometry Using Generalized Lock-in Amplifier (G-LIA): A Versatile Approach for Phase-Sensitive Sensing and Imaging

Aurélien Bruyant, Julien Vaillant, Tzu-Heng Wu, Yunlong Zhu, Yi Huang and Abeer Al Mohtar

Additional information is available at the end of the chapter

http://dx.doi.org/10.5772/66657

Abstract

A large number of interferometric setups make use of non-linear phase modulators. In the past, specific extraction methods have been proposed mostly to cover the important case of sinusoidal phase modulation with certain limits in term of signal-to-noise ratio. Recently, a detection method based on "Generalized Lock-in Amplifier" (G-LIA) was proposed to extract optimally amplitude and phase information in two-arm interferometers when nearly arbitrary phase modulations are used such as triangular or sinusoidal phase modulations. This method offers the opportunity to develop highly sensitive interferometers with simple-phase modulators such as piezo-actuated mirrors, piezo stretchers, or power-modulated laser diodes in unbalanced interferometers. Here we present the basics of the approach and we give application examples for monitoring displacement, sensing, and digital holography. The case where an amplitude modulation is also present is also detailed and discussed in the context of unbalanced interferometry and near-field nanoscopy.

Keywords: phase extraction method, unbalanced interferometry, digital holography, near-field optics, cost-effective interferometry

1. Introduction

In order to determine amplitude and phase in a two-arm interferometer, a phase modulator is often required to clearly discriminate phase changes from amplitude changes. Such operation is straightforward when the phase modulation is a linear function of time. In this case, a standard Lock-in Amplifier (LIA) gives the required information with an optimal signal to noise ratio (SNR). Unfortunately, a number of phase modulators interesting in term

of cost, achromaticity or integration offers non-linear responses, that are even sometimes coupled with unwanted amplitude modulation. A critical question that arises is "How can we extract phase and amplitude information in an optimal way when non-linear phase modulation is used?"

To solve this issue while keeping the benefits of high SNR, approaches have been proposed based on multiple lock-in detection at selected signal harmonics. These approaches were mainly employed in the case where the phase modulation is a sine function [1–6]. Such phase modulation is, for example, achieved using piezo-actuator, fiber stretchers, and other phase modulators where a sine excitation typically offers the best response. The multiple lock-in approach works fine but it is less direct and does not necessarily provide an optimal SNR or a straightforward implementation. Especially, if an amplitude modulation is present at the same frequency as that of the phase modulation. Alternately, the Generalized Lock-in Amplifier (G-LIA) technique was recently introduced [7] to solve this issue with a procedure similar to a single LIA operation. In this chapter, we first detail the principle of this method when operated in the simplest case where no amplitude modulation is present. Application is provided notably in the context of digital holography. Then we consider the case where there is an additional amplitude modulation in the signal field. The first case which is discussed is related to unbalanced interferometry where the phase modulation is achieved via a power modulation of the laser source. Finally, we also discuss the case of phase-sensitive near-field imaging.

2. Theory: introduction to G-LIA

In order to introduce the G-LIA technique, we need to provide an expression for the detected signal. We consider the simplest configuration of a 2-arm interferometer comprising a reference arm and a signal arm (cf. **Figure 1**). The system is illuminated by a monochromatic radiation. The detected signal intensity $I(t)$ can be expressed as:

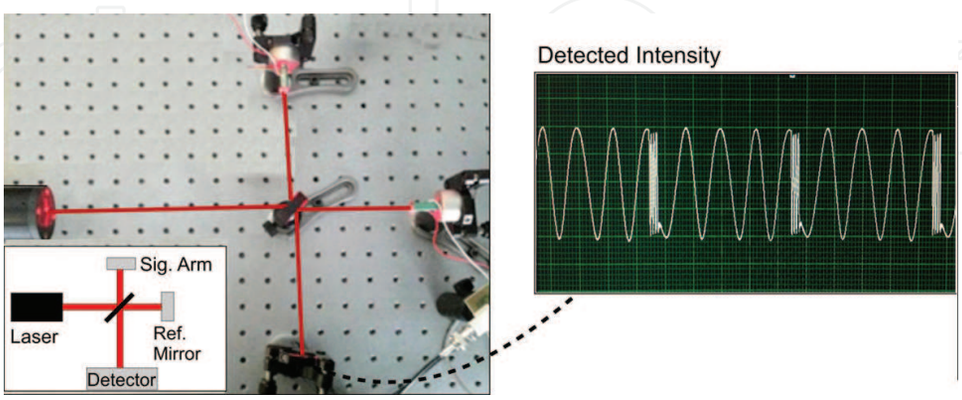

Figure 1. Pseudo-heterodyne approach. A quasi-linear phase modulation is achieved by a sawtooth modulation of the optical path using a piezo-actuated optical mirror in the reference arm. The detected intensity exhibits a sine modulation except during the flyback time of the mirror. Any phase change in the reference arm will produce a detectable phase shift of the observed quasi-sinusoidal pattern.

$$I(t) \propto E_r^2 + E_s^2 + 2mE_rE_s \cos\left(\Delta\phi(t)\right) \quad (1)$$

where E_s and E_r are, respectively, the amplitude of the field of interest and the reference field impinging on the detector. The phase difference between the two fields is $\Delta\phi(t)$ while the factor $m \leq 1$ in the interferometric term accounts for the interference contrast. Alternately, it is common to express the detected intensity as a function of the laser power P:

$$I(t) \propto P[1 + s\cos\left(\Delta\phi(t)\right)] \quad (2)$$

where s is proportional to the unknown signal amplitude E_s, considered as constant during a measurement. The unknown spatial phase ϕ_s of the signal field is also supposed to be constant during the measurement although a phase modulator can be included inside the signal arm. Any time dependence in $\Delta\phi(t)$ is therefore arbitrarily considered as coming from the reference field:

$$\Delta\phi(t) = \phi_R(t) - \phi_S \quad (3)$$

From the expression of I given by Eq. (2), different strategies can be proposed in order to recover amplitude and phase information. In order to extract the two unknowns (s, ϕ_S) from the signal $I(t)$, the phase of one of the two beams can be modulated in time by a frequency shifter or another phase modulator. When the time dependence is linear $\phi_r(t) \propto t$ as in the former case, (s, ϕ_S) are precisely determined by a Lock-in Amplifier (LIA) locked at the single frequency component present in $I(t)$. For other functions of time such as a sine waveforme (i.e. $\phi_R = \alpha \sin \Omega t$, where a is the modulation depth), the use of a conventional LIA is less trivial as the signal information is typically spread over a number of frequency components ($n\Omega/2\pi$) having different weights. The G-LIA method was introduced to handle such cases, while keeping an extraction procedure very similar to a LIA. Hereafter, the two approaches are provided to highlight the similitudes and differences.

2.1. Amplitude and phase determination using a standard LIA

2.1.1. Case of linear phase modulation (LIA)

Considering the general Eq. (2), the use of LIA is direct when $\Delta\phi(t)$ is linearly modulated by $\phi_R(t) = \Omega t = 2\pi\Delta F t$, where the phase modulation rate Ω can be induced in different ways. These ways include notably the use of a frequency shifter in one of the two arms (where ΔF is the frequency shift), a linear translation of one of the mirror (where ΔF is the associated Doppler shift), or a linear variation of the laser frequency[1] if the two arms are unbalanced. Amongst the cited methods, heterodyne measurement based on the use of frequency shifters is often considered as more favorable as a purely linear displacement of the mirror is hardly achievable in practise without alignment or coherence issues, while unbalanced

[1] In this case ΔF is function of the unbalance, that is, the optical path difference.

interferometry is subject to noise [8] induced by small wavelength fluctuation typically related to temperature drifts.

The two unknowns (s, ϕ_S) are simply the amplitude and phase of the sine waveform present in Eq. (1) which is modulated at the frequency shift ΔF. This determination is optimally carried out by a dual-output (X, Y) LIA locked at the frequency ΔF that is precisely provided by the modulator driver. Depending on the output, the detected signal I is multiplied by an in-phase or a quadrature sinusoids modulated at the same angular frequency ΔF and it is averaged over a time t_{int}:

$$X(I) = \frac{1}{t_{int}} \int_0^{t_{int}} I \ \cos(\Omega t) dt \propto s \ \cos(\phi_S) \tag{4}$$

$$Y(I) = \frac{1}{t_{int}} \int_0^{t_{int}} I \ \sin(\Omega t) dt \propto s \sin(\phi_S) \tag{5}$$

From these two outputs, the quantities $s \propto \sqrt{X^2 + Y^2}$ and $\phi_S = a\tan 2(X, Y)$ are obtained with a signal to noise ratio that can be increased using longer integration time. We note that the two in-phase and quadrature sine waveforms are the *LIA reference signals* built from the frequency shift precisely provided to the LIA. If the LIA is not locked exactly at the angular frequency Ω, the measured values of ϕ_s will drift in time, while the extracted signal amplitude will decay for long integration time.

2.1.2. Case of a non-linear phase modulation (LIA)

Achieving ϕ_r (t) $\propto$ t is not possible for a number of phase modulators, notably because they have a finite range of phase modulation. Pseudo-heterodyne approaches were proposed long ago to circumvent this problem [9] by using a sawtooth modulation of the optical path, where the peak to peak amplitude of the sawtooth corresponds to an integer number of times 2π in term of phase. The approach is illustrated by **Figure 1**, in the case where the phase ramp is achieved by a piezo-actuated mirror in a balanced interferometer.

As can be seen, the detected intensity mimics the sinusoidal beating observed in heterodyne setups. Such approach is not widely used since errors are induced during the flyback time on the sawtooth edges, especially if the modulation is fast.

As mentioned, the use of sine modulation $\phi_R = \alpha \sin \Omega t$ is regarded as much more desirable as most of the modulator can operate better and faster when they are sinusoidal excited. It was early highlighted in this context [10] that for such modulation, the Fourier spectrum of the signal has harmonic sidebands coming from the interferometric term $I_{mod} \propto P\ s \cos(\Delta\ \phi\ (t))$ in Eq. (2), as shown in **Figure 2**.

The amplitudes of these frequency components are obtained by developing the term in $I_{mod} \propto P$ [cos (ϕ_s) cos (ϕ_R) + sin(ϕ_s) sin (ϕ_R)] and using the Jacobi-Anger expansion of cos (ϕ_R) (even

http://dx.doi.org/10.5772/66657

harmonics) and sin (ϕ_R) (odd harmonics) [11]. From this expansion, we see that a LIA locked at an angular frequency harmonics mΩ, with $m \neq 0$, gives:

$$X_m(I) \propto s\cos(\phi_S)\begin{vmatrix} J_m(a) & for\ m\ even \\ 0 & for\ m\ odd \end{vmatrix} \tag{6}$$

$$Y_m(I) \propto s\ \sin(\phi_S)\begin{vmatrix} 0 & for\ \ m\ even \\ J_m(a) & for\ m\ odd \end{vmatrix}, \tag{7}$$

where J_m (a) is the m-th Bessel function. The amplitude and phase can then be extracted using both odd and even harmonics, for example, using $s \propto \sqrt{X_1^2/J_1^2(a) + Y_2^2/J_2^2(a)}$ and $\phi_S = a\tan 2\left(X_1/J_1(a),\ Y_2/J_2(a)\right)$.

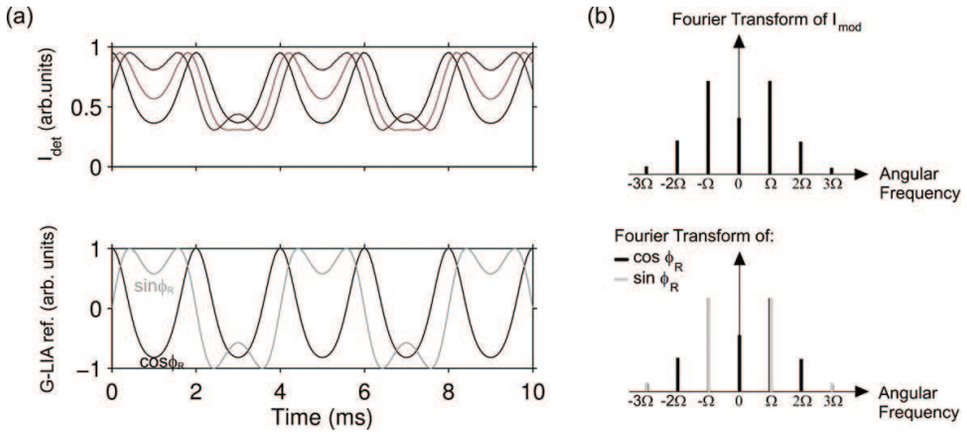

Figure 2. Signals in the case of a sinusoidal phase modulation. (a) Top: example of detected intensity for different signal phases. Bottom: corresponding reference functions. (b) Schematic example of Fourier transform of and associated references and in the case of an arbitrary sine phase modulation and $\phi_s = \pi/4$.

When only two harmonics m = (1, 2) are used, caution must be exercised in the choice of the modulation depth a in order to maximize the power density on the selected harmonics. The optimum value of a in this case is a = 2.19 rad (maximum of J_1 $(a)^2 + J_2(a)^2$).

2.2. G-LIA method

The main benefit of the G-LIA method is that all the weighted harmonics are used to retrieve phase and amplitude with an operation similar to that of a LIA. To introduce this method, we also remark that the interferometric term $I_{mod} \propto P\ s\ \cos(\Delta\phi(t))$ in Eq. (2) can be expressed as $I_{mod} \propto P\ s$ [cos (ϕ_s) $C(t)$ + sin (ϕ_s) $S(t)$], with $C(t) = cos(\phi_R)$ and $S(t) = sin(\phi_R)$. From this expression, it appears that $C(t)$ and $S(t)$ can be used as relevant reference signals within a modified LIA having the two following outputs:

$$X_{\phi R}(I_{mod}) = \frac{1}{t_{int}} \int_0^{t_{int}} I_{mod} C(t)\, dt = < I_{mod} C(t) >, \tag{8}$$

$$Y_{\phi R}(I_{mod}) = \frac{1}{t_{int}} \int_0^{t_{int}} I_{mod} S(t) dt = < I_{mod} S(t) >, \tag{9}$$

These references contain the same frequency components than the interferometric term since $I_{mod}(t)$ is a function of $C(t)$ and $S(t)$. These frequency components are naturally weighted so that the contribution of stronger harmonics will be favored. **Figure 2(b)** exemplifies the case where the phase modulation function is a sine function.

We note that in the particular case where $\phi_r(t) = \Omega t$, $C(t) = \cos(\Omega t)$ and $S(t)=\sin(\Omega t)$ and the G-LIA operation degenerates to that of a standard LIA. More generally, by replacing the expression of I_{mod} in Eqs. (8) and (9), we see that for any phase modulation we have:

$$X_{\phi R}(I_{mod}) \propto S[k_x * \cos(\phi_s) + k'_x * \sin(\phi_s)], \tag{10}$$

$$Y_{\phi R}(I_{mod}) \propto s[k'_y * \cos(\phi_s) + k_y * \sin(\phi_s)], \tag{11}$$

where $k_x = < C^2(t) >$, $k'_x = k'_y = \ < C(t)S(t) >$, and $k_y = \ < S^2(t) >$ are constants that can be calculated numerically or analytically for the considered phase modulation. But for most of the phase modulation functions that can be used $C(t)$ and $S(t)$ are orthogonal, that is, $k'_x = k'_y = \ < S(t)C(t) >= 0$, so that the $X_{\phi R}$ and $Y_{\phi R}$ outputs are:

$$X_{\phi R}(I_{mod}) \propto s k_x \cos(\phi_s), \tag{12}$$

$$Y_{\phi R}(I_{mod}) \propto s k_y \sin(\phi_s), \tag{13}$$

The G-LIA outputs are then similar to that of the LIA in the linear case (cf. Eqs. (4)–(5)). The difference is the presence of the additional proportionality constants k_x and k_y which need to be evaluated by calculating the average values $<C^2(t)>$ and $<S^2(t)>$, respectively. In the case of sine phase modulation $\phi_R = a \sin \Omega t$, the constants have analytical expressions obtained from the integral representations of Bessel functions and simple trigonometric developments:

$$k_x = 1 + J_0(2a) \tag{14}$$

$$k_y = 1 + J_0(2a) \tag{15}$$

where J_0 is the Bessel function of first kind. However, it is difficult to extract I_{mod} from $I(t)$ to feed the G-LIA input as it requires to precisely remove the signal and reference field intensities from the detected intensity $I(t)$. In general, it is not possible either to use directly $I(t)$ to perform the G-LIA operation described above. The reason is that for phase modulation function such as sine or triangle, the useful term I_{mod} also contains a DC component. In consequence the references $C(t)$ and/or $S(t)$ also contain a DC term so that the constant, non-interferometric term P in Eq. (2) is also detected by the G-LIA if $I(t)$ is used directly. To avoid this problem, specific phase modulation depths for which both $C(t)$ and $S(t)$ do not have a DC component

can be used.[2] For a sine phase modulation, this specific depth of modulation a corresponds to the zeros of the $J_0(a)$, for example, a = 2.405 rad. We note that there is no prejudice in term of signal to noise ratio using this a since all the harmonic contents is detected by the G-LIA operation.

Alternately, a satisfactory solution is to filter the detected intensity to remove all DC component from the signal. In fact, such operation is easy to do and is often highly desirable to directly remove the ambient light contribution in normal conditions [12]. In this case where the signal is filtered, the G-LIA operation is:

$$X_{\phi R}(\tilde{I}) = < \tilde{I}\ C(t) > \propto s\ K_x \cos(\phi_s), \tag{16}$$

$$Y_{\phi R}(\tilde{I}) = < \tilde{I} S(t) > \propto s\ K_y \sin(\phi_s), \tag{17}$$

where the $\tilde{I}$ denotes a DC-filtered quantity,[3] that is, $\tilde{I}(t) = I(t) - < I(t) >$. The new proportionality constants are $K_x = < \tilde{C}^2(t) >$ and $K_y = < \tilde{S}^2(t) >$, where $\tilde{C}(t) = C(t) - < C(t) >$ and $\tilde{S}(t) = C(t) - < C(t) >$ are used to evaluate these proportionality factors numerically or analytically.[4] Amplitude and phase are then provided by:

$$s \propto \sqrt{X_{\phi R}^2(\tilde{I})/K_x^2 + y_{\phi R}^2(\tilde{I})/K_y^2} \tag{18}$$

$$\phi_s = a\ tan\ 2\left(X_{\phi R}(\tilde{I})/K_x, Y_{\phi R}(\tilde{I})/K_y\right) \tag{19}$$

In the useful case of a sine modulation of the form $\phi_R = a \sin \Omega t$, the constants K_x and K_y have the following analytical expressions:

$$K_X = k_x - J_0^2(a) = 1 + J_0(2a) - J_0^2(a) \tag{20}$$

$$K_Y = k_y = 1 - J_0(2a) \tag{21}$$

---

[2] Amplitude and phase are then determined using: $s \propto \sqrt{X_{\phi R}^2(I)/k_x^2 + Y_{\phi_R}^2(I)/k_y^2}$ and $\phi_s = a\ tan 2(X_{\phi_R}(I)/k_x^2, Y_{\phi_R}(I)/k_y^2)$.

[3] An analog filter can be used. Alternately, it is possible to filter the DC component of the reference functions C(t) and S(t) only, or to filter both I and the references, with the same result. The operations $< \tilde{I}C(t) >$, $< I\tilde{C}(t) >$ and $< \tilde{I}\tilde{C}(t) >$ are theoretically equivalent. The interest of filtering both the signal and the references is that if the system operates at small modulation frequencies some filters may create a distortion of the modulated signal by changing the amplitudes of peaks and by creating phase shifts for the lowest frequency components. By filtering both the references and the signal, the distortion is similar for both the signal and references so that the distortion effect is cancelled out.

[4] A comment should also be made regarding the references C(t) and S(t). Building these references require the knowledge of $\phi = a \sin \Omega t$. In a number of setup ϕR can be monitored with sensors and it is then possible to take the sine and cosine of this quantity. The references can also be built numerically from the knowledge of the modulation depth a and frequency Ω, but C(t) and S(t) must be synchronized with $\phi_R = a \sin \Omega t$. In other word, we should not use an ersatz $\phi'_R = a \sin(\Omega t + \phi_o)$ as an argument for $C(t) = cos(\phi_R)$ and $S(t) = sin(\phi_R)$. If a phase shit ϕ0 exists, a phase adjustment of the references or the modulation drive signal can be made. This phase shift can be measured by the phase output of a standard LIA locked at the frequency Ω.

where the negative extra term in K_x comes from the filtering of the DC component which is not zero for $C(t)$. As shown in **Figure 3**, for certain phase modulation amplitude the two constants are identical and approximately equal to unity. This is obtained for $a \approx 2.814$ rad, but any phase modulation can be used. A better signal to noise ratio (SNR) is naturally achieved when there is no DC component in $C(t)$ and $S(t)$, since this part is filtered. These cases correspond to the zeros of $J_0(a)$ as previously mentioned (e.g. $a = 2.405$ rad), however the SNR is nearly optimum for a continuous range of values above $a = 2$ rad. Other analytical expressions can be given, for example, for a triangular modulation [7], however the constants estimation can be made numerically without difficulty for a variety of phase modulation functions.

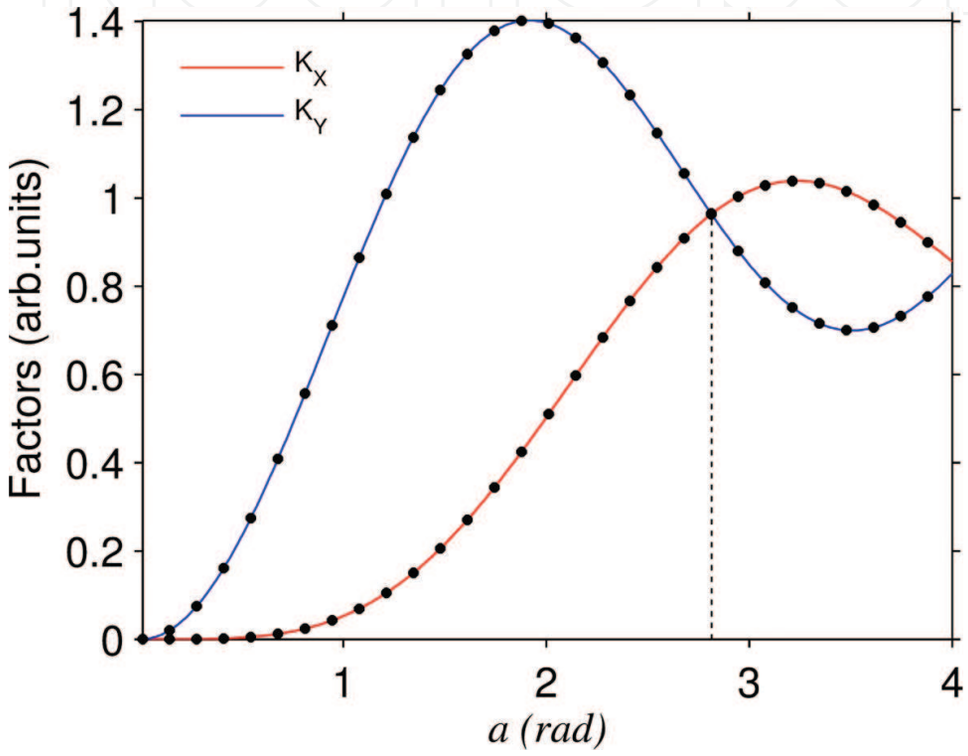

Figure 3. Proportionality factors and used in a G-LIA working with a sine phase modulation as a function of the phase modulation depth. The analytical evaluations are plotted in solid lines; the markers correspond to the numerically calculated values.

3. Application examples

In this section we review and present several results of interferometric measurements performed with the G-LIA approach described in the previous section. Results include measurement with a point detector reported elsewhere and interferometric measurement with 2D detector in the framework of holographic measurement.

3.1. Measurement with a point detector

Figure 4 shows measurement results adapted from the Ref. [7], where the G-LIA can be used with or without filtering to monitor an arbitrary displacement (here a triangle-shaped displacement).

http://dx.doi.org/10.5772/66657

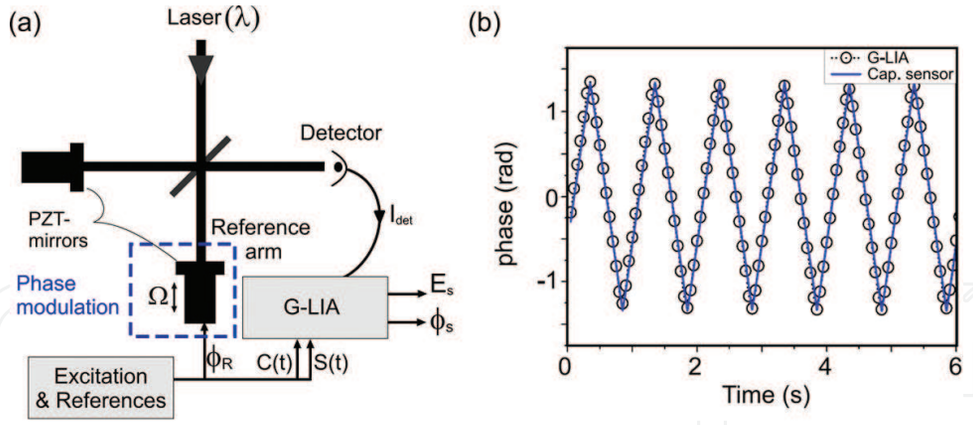

Figure 4. Interferometric measurement with a single detector. (a) Setup for displacement measurement including capacitive sensors for comparison. (b) Displacement measurement obtained with G-LIA and the capacitive sensor.

3.1.1. Displacement measurement

The setup is shown on **Figure 4(a)**. In this example, the phase modulation is a sine function $\phi_R = a \sin \Omega t$, with a modulation depth approximately equals to $a = 2.405$ rad. As explained before, with this value it is not necessary to filter the detected intensity to extract amplitude and phase from the G-LIA operations $X = \langle I\ C(t) \rangle$ and $Y = \langle I\ S(t) \rangle$. However, it is a common practise to filter the DC signal directly after the detector to get rid of the environmental light condition before acquisition in order to optimize the analog to digital conversion. In the Michelson configuration shown here, the value of a corresponds to a peak to valley oscillation of the reference mirror of about 38.3% of the wavelength. If no position sensor is present on the reference mirrors, several methods can be used to achieve the desired phase modulation depth a used in the references $C(t)$ and $S(t)$, notably by inspecting the signal $I(t)$ whose shape changes continuously with increasing value of a. Alternately the modulation depth can be precisely adjusted to recover precisely a controlled displacement of the signal mirror without affecting the amplitude output.

3.1.2. Sensing

Determining the phase rather than the amplitude is known to offer potential advantage in term of sensitivity in optical sensing systems [13]. More precisely, the phase detection coupled with surface plasmon resonance (SPR) is known to improve the measurement sensitive by one to several order of magnitude depending on the exact system geometry. Many different designs on combining interferometry or heterodyne detection on Kretschmann configuration-based SPR sensor have been done [14, 15].

Figure 5 shows the demonstration setup used in [7] to demonstrate the applicability of the G-LIA for phase sensitive sensing application. The setup is similar to that of **Figure 4(a)**, except that an I_2 gas cell was added in the reference arm. The phase modulation is still achieved with a piezo-actuated mirror and the wavelength of a laser diode emitting near 660 nm is ramped over 4pm across an absorption line of the gas. To avoid phase drift induced by the wavelength ramp, the length of the arms must be precisely balanced, since even minute wavelength fluctuation can create phase fluctuation in unbalanced interferometer. This balanced setting

can be achieved by ramping the laser diode wavelength outside an absorption band, and adjusting the position the reference mirror until the phase output of the G-LIA remains constant.

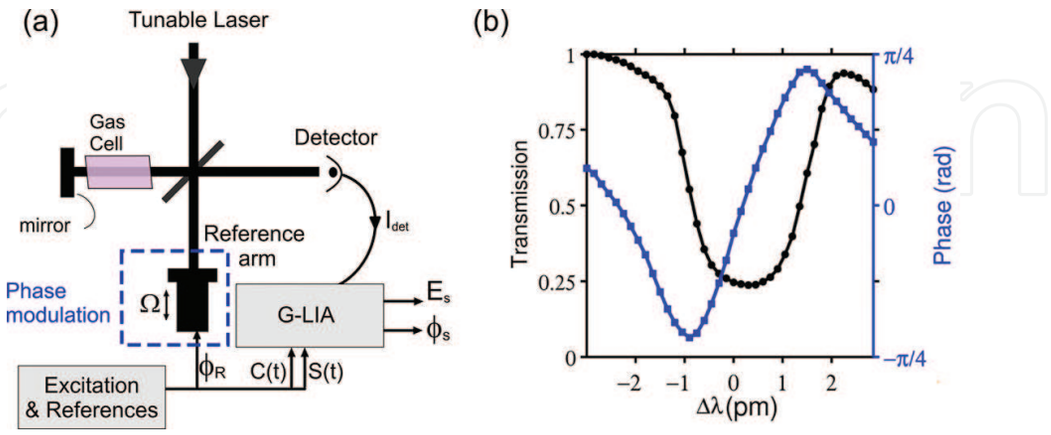

Figure 5. (a) Interferometric measurement with a single detector, applied to gas sensing. (b) Phase-sensitive detection of an absorption line. The obtained spectrum is adapted from Ref [7].

As can be seen, the phase varies more abruptly at the absorption peak center. However, the benefit of measuring the phase for monitoring a gas concentration is not clear since the amplitude has similar variation on the two sides of the absorption peak which indicates a similar sensitivity than the phase if the detection is made where the slope is maximum on the amplitude.

The interest of phase sensitive detection in SPR-based measurement is more obvious. In fact, strong plasmonic resonances can be reached by carefully adjusting the opto-geometrical parameters of the plasmonic layer in order to obtain very sharp phase variation across a resonance. One possible combination of phase sensitivity SPR bio-sensor using G-LIA for phase extraction is proposed in **Figure 6**, where a cuvette is put on a plasmonic chip to convey a fluid on the surface of a plasmonic chip. A coupling prism makes it possible to satisfy the Kretschmann condition for which the reflectivity of a p-polarized incident beam reaches a minimum corresponding the excitation of the plasmon-polariton surface mode. In order to have a stable phase, immune to wavelength fluctuations, the length of the two arms are made equal. **Figure 6(b)** presents the numerically calculated complex reflectivity as a function of the incident beam angle in the case of a glass coupling prism coated by a gold layer of thickness h covered by water and excited by a red laser. The best coupling angle is close to $\alpha = 70°$ in the provided examples.

As can be seen, the phase variation across the resonance can be made very sharp by adjusting the metal thickness h. It should be noted however that this fast variation is associated with a strong attenuation of the reflected beam and a compromise between signal level and sensitivity can be made depending on the available laser power. For example, on **Figure 6(b)** the reflection is about 1.6% for $h = 48$ nm at Kretschmann angle, but it drops to 2.5‰ for $h = 50$ nm.

http://dx.doi.org/10.5772/66657

If we consider a reasonable phase resolution of 10^{-3} rad, simple calculation show that the case h = 50 nm shown on the figure leads to sensitivity slightly better than 8×10^{-7} RIU (refractive index unit). On the other hand, if the thickness is slightly inferior, the RIU sensitivity drops rapidly (about 2×10^{-6} for h = 48 nm). To obtain a similar sensitivity with the only amplitude signal, the noise level on the amplitude measured at the maximum slope should be smaller than 10^{-3}%, which is hardly achievable.

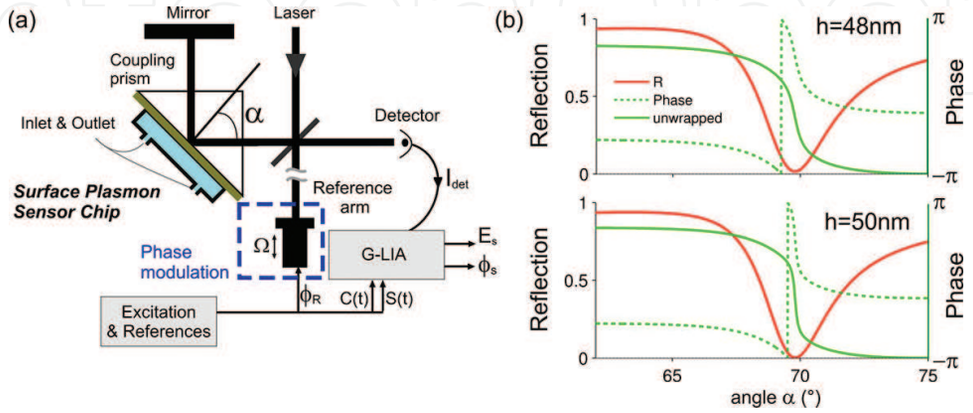

Figure 6. Example of possible experimental setup for phase sensing based on an SPR chip. (b) Simulation of the complex reflectivity (magnitude and phase) for a light beam impinging a gold layer with a thickness h as a function of the incident angle. The wavelength is 670 nm.

3.2. Digital holography

In digital holography, the holograms of a sample object are recorded on a 2D detector such as a Charge-coupled Device (CCD) or a Complementary Metal-Oxide-Semiconductor (CMOS) camera. Such system can notably be used as an optical profilometer, or for sensing applications [1, 6, 16]. **Figure 7(a)** presents the experimental setup of a lensless, compact, digital microscope working with the G-LIA extraction method.

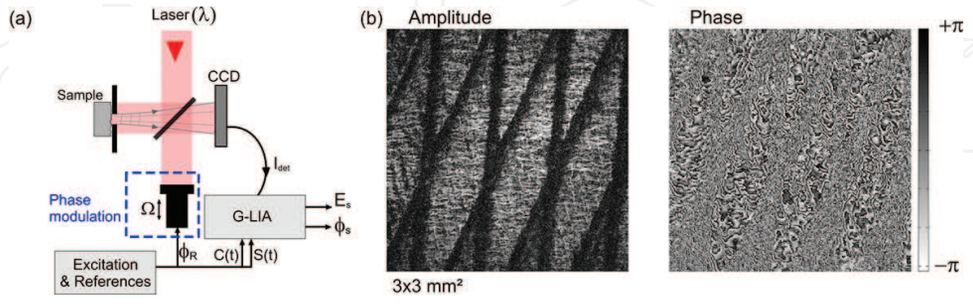

Figure 7. (a) Lensless digital holography setup. A diaphgram may be to select the central zone of interest in the sample. (b) Amplitude and phase of a grating of straight and tilted slits made in a steel surface.

In the provided example, a metallic grid of slit is imaged in amplitude and phase. The Lead Zirconate Titanate (PZT) oscillates in the reference arm at 10 Hz to generate the phase modulation function $\phi_R = a \sin \Omega t$ at a wavelength λ = 640 nm in the reference arm. During the piezo

oscillation, a video is recorded at a frame rate of 120 Hz. Then, amplitude and phase of the detected field is obtained on the camera by performing a G-LIA operation on each pixel using a program code. In this 2D case, the operation was not made in real-time because of the non-negligible processing time (In the order of 1 min or less depending on the computing resource). Once the detected complex field is retrieved, the associated plane wave spectrum can be obtained by Fourier transform. Then each plane wave can be back-propagated numerically to any position before the CCD [17], typically up to the sample plane or surface.

In this example, the raw signal $I(X,Y)$ is processed by the numeric, software-based, G-LIA, without filtering. For a correct operation it is then mandatory to use an amplitude modulation a of about 2.405 rad. **Figure 7(b)** shows the amplitude and phase of the complex field which is back-propagated up to the sample plane. As we are dealing with a rough surface, the recorded phase has a speckle-like distribution. Because the illumination direction is normal to the sample surface, the system is strongly sensitive to any out-of-plane displacement of the structure. To give an idea of the system sensitivity, the sample is slightly rotated. By subtracting the phase image before rotation to the phase image after rotation, we obtain the phase-shift associated with the out-of-plane displacements, as shown in **Figure 8**.

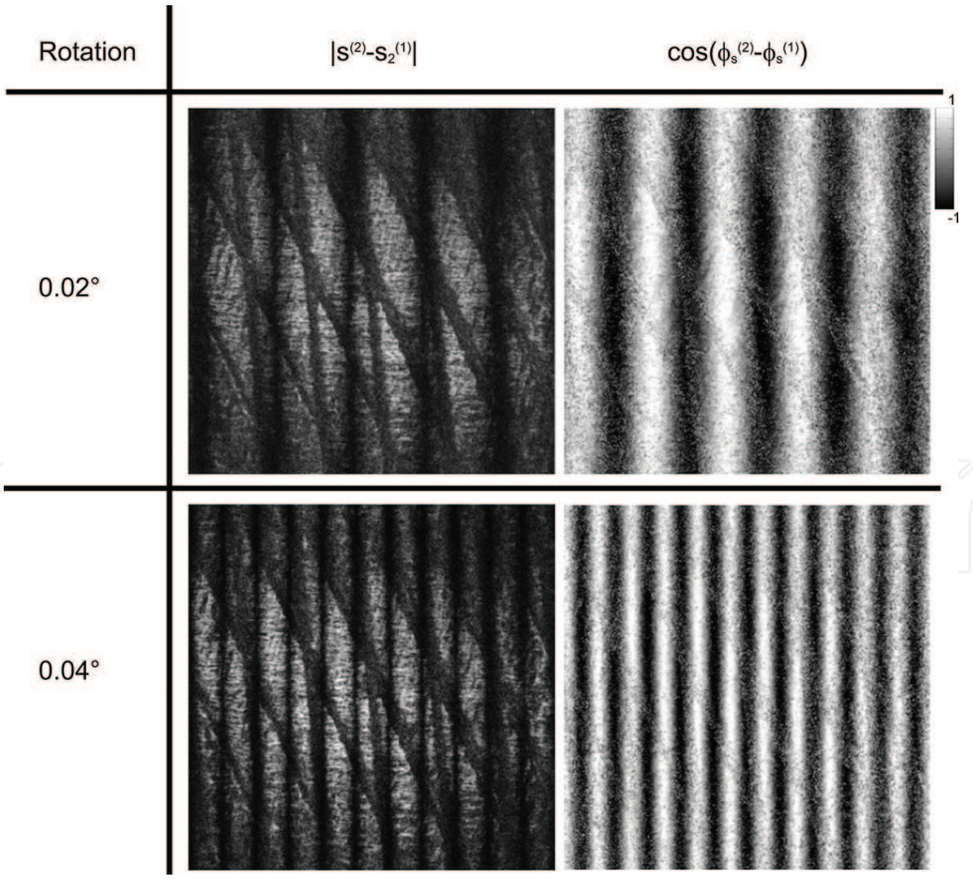

Figure 8. Effect of slight rotation on the holographic images. By subtracting the complex field after rotation $s^{(2)}(X,Y)$ from the complex field before rotation $s^{(1)}(X,Y)$, the out of plane displacement is revealed.

4. G-LIA in the case of amplitude and phase-modulated signal

In some important cases, the signal field is modulated both in phase and amplitude. The modulated term $I_{mod} \propto P\, s \cos(\Delta\phi(t))$ in the detected intensity can then be expressed as:

$$I_{mod} \propto f(t) \cos\left(\Delta\phi(t)\right) \tag{22}$$

where $f(t)$ accounts for the amplitude modulation function. We can mention two relevant examples in the context of *phase-sensitive nanoscopy* and *unbalanced interferometry*.

4.1. Unbalanced interferometry

In interferometers having a path unbalance, a phase modulation can be efficiently induced by a wavelength modulation of the emission wavelength. For this purpose a spectrally single-mode laser diode working at a central wavelength λ_0 can be used. The wavelength modulation is typically obtained by a current modulation which is associated with a power modulation. In air, the phase modulation is related to the small wavelength modulation $\delta\lambda(t)$ by: $\phi_R(t) = \frac{4\pi\Delta l\ \delta\lambda(t)}{\lambda_0^2}$, where Δl is the length difference between the two arms.

For modulation frequency below the MHz range, the change in wavelength is considered to be primarily due to a change of temperature that increases with the current. Therefore, using a sawtooth function to create a quasi-linear phase change is usually not an excellent choice, as the thermal inertia of the system prevents the wavelength to precisely follow the driving excitation. On the other hand, a sine power modulation will typically induce the desired sine wavelength and phase modulation. In this case, the detected intensity within an unbalanced interferometer is:

$$I \propto P_0\left(1 + \mu \sin(\Omega t)\right)\left(1 + s\cos(\phi_r - \phi_s)\right) \tag{23}$$

with $\phi_R(t) = a \sin(\phi_R)$, where $a = \frac{4\pi\Delta l a_\lambda}{\lambda_0^2}$ with a_λ corresponding to the depth of wavelength modulation.

It is clear that in the case where the amplitude modulation is small ($\mu \ll 1$ and $\mu \ll s$), the amplitude modulation disappears and the G-LIA method can be applied directly using the signal $\tilde{I}(t)$ where the DC component is filtered, with the references $C(t) = cos\ (\phi_R)$ and $S(t) = sin\ (\phi_R)$. The operations are identical to those given by Eqs. (16)–(21). However, while μ can be small compared to 1, the signal s of interest can also be very small in some experiments and setups so that $\mu \ll s$ cannot be satisfied in general. To see how to handle this problem, we can express the filtered intensity $\tilde{I}(t)$:

$$\tilde{I} \propto s[\cos(\varphi_r - \varphi_s)\left(\mu \sin(\Omega t) + 1\right)]_{filtered} + \mu \sin(\Omega t) \tag{24}$$

where we have normalized the detected intensity by the constant laser power factor. The brackets indicate the quantity is filtered from its DC component. We see that the main issue

comes from the modulated term outside the bracket which is independent from the signal s. A direct solution to get rid of this unwanted term is to use references without harmonic component at Ω. This is achieved by choosing $J_1(a) = 0$ (e.g. $a = 3.832$ rad). With this choice of a, the G-LIA operation given by Eqs. (16)–(24) gives excellent results provided that μ is kept reasonably small in comparison with 1 (e.g. for μ = 0.1 the maximum error on the G-LIA X and Y output is about 2%).[5] This condition is reasonably achieved in many cases. For example, if we consider a standard single mode laser diode such as a Vertical Cavity Surface Emitting Laser (VCSEL) with a tunability of 0.5 nm/mA and a bias current of 1 mA. We see that a current modulation of 4.4% is sufficient to achieve $a = 3.8$ rad for an unbalance of 10 mm at a wavelength of 850 nm. The corresponding power modulation μ depends on its $P(I)$ but will be typically smaller than 0.1.

4.1.1. Improved unbalanced configuration

Despite its advantages in term of cost, unbalanced interferometry is not currently widely used. The main reason is also related to the extreme sensitivity of the system to minute wavelengths changes. **Figure 9(a)** represents a compensation scheme to solve this issue. The idea is to illuminate the interferometer with a linear polarization at 45° with respect to the horizontal and vertical axis and to discriminate the two s and p polarization using polarization beam splitters. An additional signal arm is equipped with a fixed mirror in order to measure the phase fluctuation induced by any wavelength drifts in time. The light impinging on this mirror is s-polarized and is selectively detected by the photodiode PD1, using a polarization beam splitter in reflection. On the other hand, the p-polarized light impinging on the piezo-actuated mirror is reflected back onto the second photodiode (PD2). Both amplitude and phases are recorded with the above described G-LIA operation.

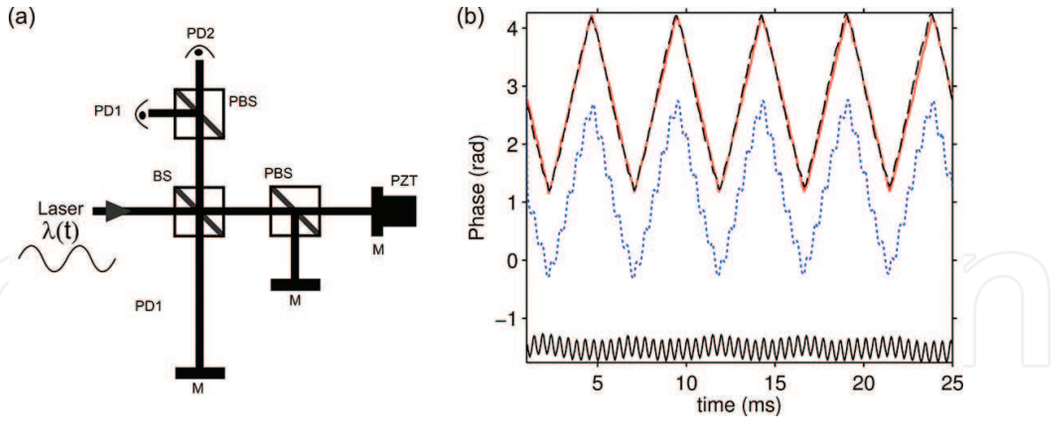

Figure 9. (a) Unbalanced interferometer with an extra arm for wavelength drifts compensation. The sine phase modulation is induced by a power modulation of the VCSEL laser source. BS: Beam splitter. (b) Actual displacement of the piezo actuated mirror (red); measured displacement without drift compensation (dotted blue); phase fluctuation induced by the intentional wavelength fluctuation (black line), and final measurement (dashed black line) obtained by subtracting the black line to the blue dotted line.

[5]We note that the cases where μ is too large to be neglected can be handled exactly without approximation but it requires to know μ in order to determine analytically or numerically all the coefficients of the G-LIA outputs (4 in this case). In general, the percentage of power modulation μ can be measured without difficulty. The condition J1(a) = 0 is still required.

http://dx.doi.org/10.5772/66657

Figure 9(b) shows a controlled triangular displacement which is correctly determined despite the presence of intentional wavelength drifts. In this experiment, the wavelength of the VCSEL is driven sinusoidally at about 10 kHz to create the phase modulation. The important wavelength drifts are artificially created by adding a low frequency sine to this excitation signal. The compensation is obtained by plotting the phase of the p-polarized light minus the phase of the s-polarized light which is coming from the fixed mirror. Both signal phases are obtained by the G-LIA method with a approximately equal to 3.83 rad.

Such system is really interesting in term of performance since VCSELs are very affordable laser sources that can be driven at very sinusoidally at very high speed. In the described experiment the phase modulation frequency was only limited by the acquisition card used to perform the G-LIA measurement.

4.2. Phase-sensitive nanoscopy

A modulation of the amplitude at an angular frequency Ω_A can be introduced in the signal arm to discriminate the amplitude-modulated signal from other unwanted contributions able to interfere with the reference field. This is the case in near-field nanoscopy where the signal light is coming from a near-field probe in interaction with a surface, oscillating at an angular frequency Ω_{probe}. The situation is depicted in **Figure 10**.

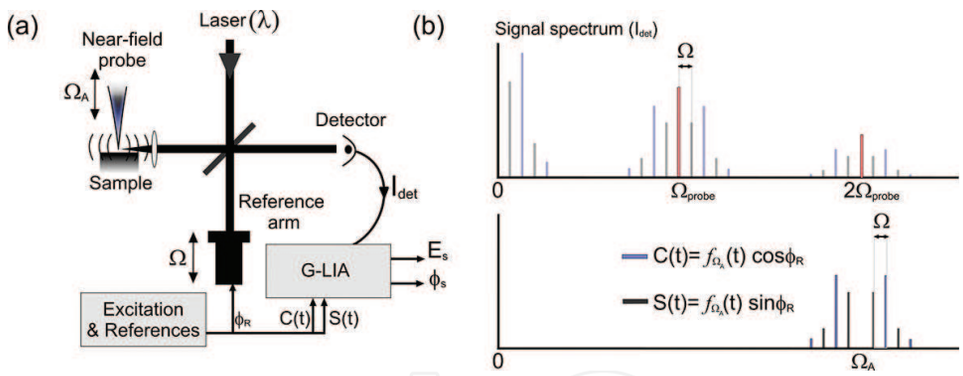

Figure 10. Phase-sensitive nanoscopy experiment based on G-LIA, where the phase modulation is $\varphi_R = a \sin \Omega t$. (a) Basic setup. (b) Illustration of the frequency spectra of (top) the detected intensity and (bottom) the references signal used in the extraction process. In this example $\Omega_A = 2\Omega_{probe}$. The condition (e.g. $a = 2.405$ rad) removes the unwanted peaks from the references.

In **Figure 10**, the near-field head is included in the signal arm of a Michelson interferometer. Alternately the near-field microscope can be used in the signal arm of a Mach-Zhender which is well adapted to the characterization of waveguiding photonic devices as in [18–20]. Here, the sample is scanned under a nano-tip which is precisely positioned in the focus spot of an objective lens. The light backscattered by the oscillating probe operating in tapping mode contains information on the local optical properties of the sample. This backscattered light can have a rich harmonic content due to its near-field interaction with a sample. The amplitude modulation function appearing in I_{mod} is therefore $f(t) = cte + s_1\ cos(\Omega_{probe}t + \Phi_1) + s_2\ cos(2\Omega_{probe}t + \Phi_2) + \ldots$

We note that I_{mod} in this case refers to the interference term between the *near-field signal* from the probe and the phase-modulated *reference signal*. However other parasitic fields can be backscattered by the probe-sample system. When using a standard, cantilevered, AFM probe, the oscillation amplitude is typically larger than the probe radius. In this case it is often interesting to detect the contribution from a higher harmonics $\Omega_A = k\Omega_{probe}$ as the unwanted part of the light which is modulated by the shaft of the probe (rather than the apex) only contributes to the first harmonic(s). This unwanted contribution modulated by the probe shaft can be referred as *modulated background contribution* (MBC) in contrast with the *unmodulated background contribution* (UBC) coming, for example, from the sample backscattering (nano-dusts, roughness, …) which is also unwanted. In less stringent configurations, especially when the oscillation is small compared to the tip radius (the near field varies almost linearly on the excursion of the probe), the MBC is not perceived[6] while keeping $k=1$.

As shown in **Figure 10(b)**, because of the interference between the probe signal and the reference field, the signal is split into sidebands at $k\Omega_{probe} \pm p\Omega$ where Ω characterize the phase modulation frequency. In order to collect the information spread throughout all these side-bands, the G-LIA can use the following references:

$$C(t) = f_{\Omega A}(t)cos(\phi_R t) \tag{25}$$

$$S(t) = f_{\Omega_A}(t)sin(\phi_R t) \tag{26}$$

where $f\Omega_A(t) = cos(\Omega_A t + \psi)$ is the amplitude carrier at the frequency of interest Ω_A. But even in this favorable case where the MBC is easily excluded, the UBC can be especially detrimental and has been described by several authors. UBC however can be efficiently removed with interferometric detection. As noted elsewhere, the UBC is perceived because the unmodulated background interferes with the modulated signal from the tip on the detector creating signal peaks at the harmonics frequencies $k\Omega_{probe}$. Therefore a direct solution consists in excluding the frequencies $\Omega_A = k\Omega_{probe}$ from the references $C(t)$ and $S(t)$. In the case of a sine modulation, the condition $a = 2.405$ rad ($J_0(a) = 0$) is sufficient to exclude the unwanted frequencies component by removing the possible DC contribution in $\cos(\phi_R t)$.

First examples of phase-sensitive near-field imaging based on G-LIA can be found in Ref. [7]. In **Figure 11**, a simple demonstration experiment is made by using a bare tuning oscillating fork to modulate part of the signal at an angular frequency Ω_A. The trace of the experimentally detected signal intensity exhibits clearly a slow modulation due the phase modulation ($\phi_R = a$ sin Ωt with a frequency of 1 kHz) as well as a sine amplitude oscillation at the oscillation frequency of the tuning fork Ω_A (at about 32 kHz). An additional coverglass can be added to

[6]Such case occurs when using elongated probes like tungsten probes, mounted on tuning fork working in tapping mode. The elongated shape minimizes the possible modulation of the background light, while an oscillation amplitude of few nanometers can also prevent a detectable modulation of the background light. In some other case where a Mach-Zehnder interferometer is used, only the apex of the probe can be illuminated (e.g.when imaging waveguiding structures). In general, reducing the amplitude of modulation of the probe reduces the background contributions more efficiently than the near-field contribution.

http://dx.doi.org/10.5772/66657

check the system immunity to UBC. In this example, the references are those given by Eqs. (25)–(26) with $f\Omega_A(t) = cos(\Omega_A t + \psi)$ where ψ is adjusted to be in phase with the fork oscillation, resulting in a maximized amplitude signal (not shown here). With a = 2.405 rad to exclude the UBC, the two G-LIA outputs provide:

$$X =< I(det) * C(t) > \propto k_x s_1 \cos(\phi_s), with\ k_x = \langle C^2(t) \rangle \tag{27}$$

$$Y =< I(det) * C(t) > \propto k_y s_1 \cos(\phi_s)\ with\ k_y = \langle S^2(t) \rangle \tag{28}$$

where s_1 corresponds to the amplitude of signal field modulated at Ω_A. For a sine phase modulation, an analytical expression can be derived for the proportionality constants k_x and k_y.These expressions can be found in the summary table given in Appendix A.

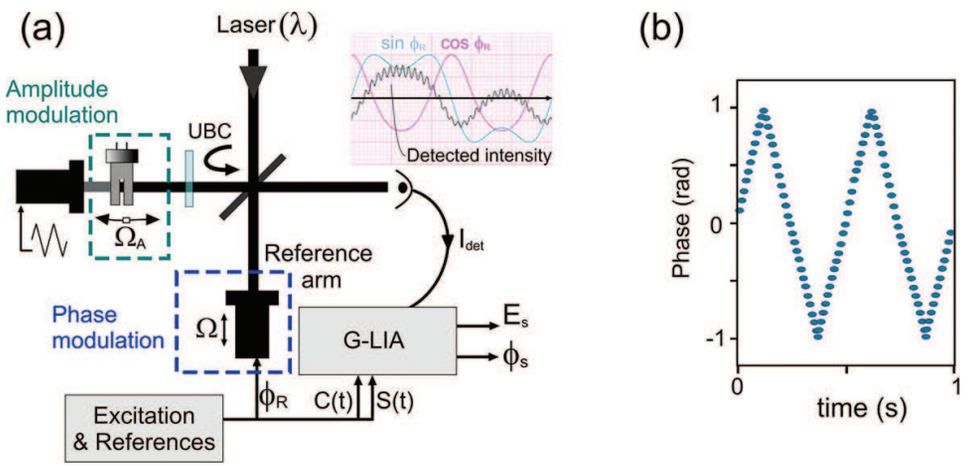

Figure 11. (a) Demonstration setup with $\phi_R = a \sin \Omega t$. An UBC can be added via a glass coverslip in the signal arm. (b) Recovered signal phase for a triangular displacement of the signal mirror.

Figure 11(b) shows the phase determined with this method when a triangular phase modulation having a peak to peak phase modulation depth of about 2.0 rad is induced by the signal mirror. The signal phase is precisely retrieved.

The value of ψ includes the mechanical phase shift existing between the driving signal and the actual motion of the fork. In fact, in a near-field experiment, this shift can vary from one position to another on the sample depending on the material in interaction with the probe. Depending on the system, the value of ψ in $f\Omega_A(t) = cos(\Omega_A t + \psi)$ is not necessarily known if only the driving signal is accessible. We note that the retrieved optical phase value is not affected by the value of ψ, which only affects the amplitude, but the SNR can be strongly decreased if we omit ψ.

If ψ is unknown, the G-LIA can be applied twice to solve this issue with two quadrature amplitude modulation functions. In other word, we can calculate for outputs signals $(X, Y, X', Y') =< I{*}reference(t) >$, using, respectively, the following references:

$$C(t) = cos\Big(\Omega_A(t)\Big)cos(\phi_R t) \tag{29}$$

$$S(t) = cos\Big(\Omega_A(t)\Big)sin(\phi_R t) \tag{30}$$

$$C'(t) = sin\Big(\Omega_A(t)\Big)cos(\phi_R t) \tag{31}$$

$$S'(t) = sin\Big(\Omega_A(t)\Big)sin(\phi_R t) \tag{32}$$

The four outputs (X, Y, X', Y') can be evaluated numerically or analytically, they provide, respectively, $< C(t)^2 > cos(\phi_s)$, $< S(t)^2 > sin(\phi_s)$, $< C'(t)^2 > cos(\phi_s)$, $< S'(t)^2 > sin(\phi_s)$ whose analytical expressions are given in Appendix A for the sine phase modulation $\phi_R(t)$.

5. Conclusion

We have detailed the principle of the G-LIA method, first in the case of pure phase modulations then in the case where the amplitude of the signal is also modulated. For pure phase modulations, the interest of the approach was illustrated in different contexts: position monitoring, sensing, and digital holography. In these experiments, the non-linear phase modulation was achieved by mirrors mounted on sinusoidally driven piezo-actuators. In this case, the main advantage of the G-LIA is to extract amplitude and phase information directly from all the harmonic contents created by the phase modulation function. While the examples only considered sine phase modulation functions which is often the most desirable one, the G-LIA also provides a unified treatment to handle arbitrary phase modulation function.

We have also detailed the case where an amplitude modulation can be present. This is notably the case in unbalanced interferometry where a non-negligible amplitude modulation can be perceived at the same frequency than the phase modulation. Experimentally, we considered the case of unbalanced interferometers where a fast sine phase modulation is provided by a current-driven single mode laser diode. A simple yet efficient setup was described to neutralize the impact of wavelength fluctuation on the system. Such approach offers the opportunity to develop simple and cost-efficient system without sacrificing precision. Finally, we discussed the case where the signal of interest is modulated in amplitude at a frequency different from that of the phase modulation. This case was detailed in the context of phase sensitive SNOM, where the low available signal requires to exploit all the available sidebands induced by the phase modulation. Notably, the condition to cancel the effect of the unmodulated background light was presented and attention was paid to the impact of the mechanical phase of the oscillating probe.

Appendix A

The table (**Figure 12**) provides a summary of case handled by the G-LIA method.

Modulation Functions		References	G-LIA on I_{det}		G-LIA on $\tilde{I}_{det}$
Phase $\phi_R(t)$	Amplitude $f(t)$	(X, Y)	(k_x, k_y)	Condition	(K_x, K_y)
Ωt	-	$C(t) = \cos\phi_R$, $S(t) = \sin\phi_R$	1,1	-	1,1
$a \sin(\Omega t)$	-		$1+J_o(2a)$, $1-J_o(2a)$	$J_o^2(a) \approx 0$	$k_x-2J_o^2(a)$ k_y
$a\ Tr(\Omega t)$	-		$1+2\,sinc(2a)$, $1-2sinc(2a)$	$sinc^2(a) \approx 0$	$k_x-sinc^2(a)$ k_y
other	-		analytic or numeric evaluation of $\langle C^2(t)\rangle$ and $\langle S^2(t)\rangle$	No DC term in the references	analytic or numeric evaluation of $\langle \tilde{C}^2(t)\rangle$ and $\langle \tilde{S}^2(t)\rangle$
Ωt	$\cos(\Omega_\Lambda t+cte)$ cte: known	$C(t) = 2f(t)\cos\phi_R$, $S(t) = 2f(t)\sin\phi_R$	1,1		
$a \sin(\Omega t)$			$1+g(a)$, $1-g(a)$		
other	other		analytic or numeric evaluation of $\langle C^2(t)\rangle$ and $\langle S^2(t)\rangle$		
Modulation Functions		References	G-LIA on I_{det}		
Phase $\phi_R(t)$	Amplitude	(X, Y, X', Y')	(k_x, k_y, k_x', k_y')		
$a \sin(\Omega t)$	$\cos(\Omega_\Lambda t+\psi)$ ψ unknown	$\cos(n\Omega t)\cos\phi_R$, $\cos(n\Omega t)\sin\phi_R$, $\sin(n\Omega t)\cos\phi_R$, $\sin(n\Omega t)\sin\phi_R$	$(1+g(a))\cos\psi$, $(1-g(a))\cos\psi$, $-(1+g(a))\sin\psi$, $-(1-g(a))\sin\psi$		

$g(a)=J_{2n}(2a)+J_o(2a)$

$n=\Omega_\Lambda/\Omega$ is preferentially large

The case n=1 is treated separately

For a sine phase modulation, an eventual UBC is canceled if $J_o(a)=0$ (e.g. a=2.405 rad)

The 4 unknowns (Es, ϕ_s, $\cos\psi$, $\sin\psi$) are retrieved from the 4 outputs X, Y, X', Y'

Figure 12. Summary table.

Author details

Aurélien Bruyant*, Julien Vaillant, Tzu-Heng Wu, Yunlong Zhu, Yi Huang and Abeer Al Mohtar

*Address all correspondence to: aurelien.bruyant@utt.fr

ICD-LNIO, Université de Technologie de Troyes, Troyes, France

References

[1] O. Sasaki, and H. Okazaki. Sinusoidal phase modulating interferometry for surface profile measurement. Appl. Opt. 1986;**25**(18):3137–3140. DOI: 10.1364/AO.25.003137

[2] O. Sasaki, and H. Okazaki. Analysis of measurement accuracy in sinusoidal phase modulating interferometry. Appl. Opt. 1986;**25**(18): 3152–3158. DOI: 10.1364/AO.25.003152

[3] O. Sasaki, T. Suzuki, and K. Takahashi. Sinusoidal phase modulating laser diode interferometer with feedback control system to eliminate external disturbance. Opt. Eng. 1990;**29** (12):1511–1515. DOI: 10.1117/12.55754

[4] G. He, and X. Wang. Real-time micro-vibration measurement in sinusoidal phase-modulating interferometry. Optik. 2009;**120**(3):101–105. DOI: 10.1016/j.ijleo.2007.05.010.

[5] Z. Li, X. Wang, P. Bu, B. Huang, and D. Zheng. Sinusoidal phase-modulating laser diode interferometer insensitive to the intensity modulation of the light source. Optik. 2009;**120** (16):799–803. DOI: 10.1016/j.ijleo.2008.03.015

[6] E. Bo, F. Duan, C. Lv, F. Zhang, and F. Feng. Sinusoidal phase modulating interferometry system for 3D profile measurement. Opt. Laser Technol. 2014;**59**:137–142.

[7] A. Al Mohtar, J. Vaillant, Z. Sedaghat, M. Kazan, L. Joly, C. Stoeffler, J. Cousin, A. Khoury, and A. Bruyant. Generalized lock-in detection for interferometry: application to phase sensitive spectroscopy and near-field nanoscopy. Opt. Express 2014;**22**(18):22232–22245. DOI: 10.1364/OE.22.022232

[8] G. Economou, R. Youngquist, and D. Davies. Limitations and noise in interferometric systems using frequency ramped single-mode diode lasers. J. Lightwave Technol. 1986;**4** (11):1601–1608. DOI: 10.1109/JLT.1986.1074672

[9] D.A. Jackson, A.D Kersey, M. Corke, and J.D.C. Jones. Pseudoheterodyne detection scheme for optical interferometers. Electron Lett. 1982;**18**(25–26):1081. DOI: 10.1049/el:19820740

[10] A. Dandridge, A. Tveten, and T. Giallorenzi. Homodyne demodulation scheme for fiber optic sensors using phase generated carrier. IEEE Trans. Microwave Theory Tech. 1982;**30** (10): 1635–1641. DOI: 10.1109/JQE.1982.1071416

[11] G.B. Arfken, H.J. Weber, and F.E. Harris. Mathematical methods for physicists: a comprehensive guide. Academic Press, Waltham, USA & Kidlington, UK; 2011.

[12] L. Shen, J.A. Hagen, and I. Papautsky. Point-of-care colorimetric detection with a smartphone. Lab Chip. 2012;**12**(21):4240–4243. DOI: 10.1039/C2LC40741H

[13] Y.H. Huang, H.P. Ho, S.Y. Wu, S.K. Kong. Detecting phase shifts in surface plasmon resonance: a review. Adv. Opt. Technol. 2011. DOI: 10.1155/2012/471957

[14] C.M. Wu, Z.C. Jian, S.F. Joe, and L.B. Chang. High-sensitivity sensor based on surface plasmon resonance and heterodyne interferometry. Sens. Actuators B. 2003;**92**(1):133–136. DOI: 10.1016/S0925-4005(03)00157-6

[15] W. Yuan, H.P. Ho, C.L. Wong, S.K. Kong, and C. Lin. Surface plasmon resonance biosensor incorporated in a Michelson interferometer with enhanced sensitivity. IEEE Sensors J. 2007;**7**(1):70–73. DOI: 10.1109/JSEN.2006.884982

[16] B. Javidi, and E. Tajahuerce. Three-dimensional object recognition by use of digital holography. Opt. Lett. 2000;**25**(9):610–612. DOI: 10.1364/OL.25.000610

[17] K.A. Stetson. Mathematical refocusing of images in electronic holography. Appl. Optics. 2009;**48**(19):3565–3569. DOI: 10.1364/AO.48.003565

[18] B. Dagens, M. Février, P. Gogol, S. Blaize, A. Apuzzo, G. Magno, R. Mégy, and G. Lerondel. Direct observation of optical field phase carving in the vicinity of plasmonic metasurfaces. Nano Lett. 2016. DOI: 10.1021/acs.nanolett.6b00435

[19] X. Wu, L. Sun, J. Wang, and Q. Tan. Real-time phase error compensation in phase sensitive scanning near-field optical microscopy. Appl. Optics. 2015;**54**(19):6128–6133. DOI: 10.1364/AO.54.006128

[20] N. Rotenberg, and L. Kuipers. Mapping nanoscale light fields. Nature Photon. 2014;**8**(12):919–926. DOI: 10.1038/nphoton.2014.285

IntechOpen